JOURNAL OF BACTERIOLOGY, May 2009, p. 3339–3349 Vol. 191, No. 10
0021-9193/09/$08.00+0 doi:10.1128/JB.01782-08


# Surface Location of Individual Residues of SlpA Provides Insight into the *Lactobacillus brevis* S-Layer[▽]

Heikki Vilen,[1] Ulla Hynönen,[1] Helga Badelt-Lichtblau,[2] Nicola Ilk,[2] Pentti Jääskeläinen,[3] Mika Torkkeli,[4] and Airi Palva[1]*

*Department of Basic Veterinary Sciences, Division of Microbiology and Epidemiology, P.O. Box 66, FIN-00014 University of Helsinki, Helsinki, Finland[1]; Center for NanoBiotechnology, BOKU University of Natural Resources and Applied Life Sciences Vienna, A-1180 Vienna, Austria[2]; Centre of Excellence in Computational Complex Systems Research, Department of Biomedical Engineering and Computational Science, Faculty of Information and Natural Sciences, Helsinki University of Technology (HUT), P.O. Box 9203, FIN-02015 HUT, Espoo, Finland[3]; and Department of Physics, Division of Materials Physics, P.O. Box 64, FIN-00014, University of Helsinki, Helsinki, Finland[4]*

Received 19 December 2008/Accepted 11 March 2009

**Bacterial surface layer (S-layer) proteins are excellent candidates for in vivo and in vitro nanobiotechnological applications because of their ability to self-assemble into two-dimensional lattices that form the outermost layer of many *Eubacteria* and most *Archaea* species. Despite this potential, knowledge about their molecular architecture is limited. In this study, we investigated SlpA, the S-layer protein of the potentially probiotic bacterium *Lactobacillus brevis* ATCC 8287 by cysteine-scanning mutagenesis and chemical modification. We generated a series of 46 mutant proteins by replacing single amino acids with cysteine, which is not present in the wild-type protein. Most of the replaced amino acids were located in the self-assembly domain (residues 179 to 435) that likely faces the outer surface of the lattice. As revealed by electron microscopy, all the mutant proteins were able to form self-assembly products identical to that of the wild type, proving that this replacement does not dramatically alter the protein conformation. The surface accessibility of the sulfhydryl groups introduced was studied with two maleimide-containing marker molecules, TMM$(PEG)_{12}$ (molecular weight [MW], 2,360) and AlexaFluor488-maleimide (MW = 720), using both monomeric proteins in solution and proteins allowed to self-assemble on cell wall fragments. Using the acquired data and available domain information, we assigned the mutated residues into four groups according to their location in the protein monomer and lattice structure: outer surface of the lattice (9 residues), inner surface of the lattice (9), protein interior (12), and protein-protein interface/pore regions (16). This information is essential, e.g., in the development of therapeutic and other health-related applications of *Lactobacillus* S-layers.**

Bacterial surface layers (S-layers) are cell envelope structures ubiquitously found in gram-positive and gram-negative bacteria as well as in *Archaea*. S-layers are composed of identical (glyco)protein subunits with a molecular mass in the range of 40 to 200 kDa. The proteins self-assemble into two-dimensional crystalline structures with oblique (p1, p2), square (p4), or hexagonal (p3, p6) symmetry, covering the entire cell surface. The subunits are held together and attached to the underlying cell wall by noncovalent interactions and they have an intrinsic ability to spontaneously form regular layers in solution and on solid supports (24). S-layers have been shown to have roles in the determination and maintenance of cell shape as virulence factors, as mediators of cell adhesion, and as regulators of immature dendritic and T cells. Moreover, they can also function as a protective coat, molecular sieve, murein hydrolase, and ion trap (4, 8, 13, 17, 19, 25, 29).

S-layer proteins have several properties that make them an attractive target for the development of nanobiotechnological applications both in vivo and in vitro. In particular, a high number of protein subunits are displayed at the bacterial cell surface. Moreover, the protein subunits are able to spontaneously self-assemble into a regularly arranged lattice structure both in solution and on solid supports (1, 27, 30, 31). However, despite the high prevalence of S-layers in nature, their molecular structure remains poorly elucidated. In particular, knowledge about the spatial organization of amino acid residues in S-layer proteins or the interactions between these residues and other subunits is limited. The poor solubility of protein assemblies and the absence of stoichiometrically defined oligomers have hindered attempts to apply nuclear magnetic resonance or hydrogen/deuterium exchange mass spectroscopy. In addition, the intrinsic property of S-layer proteins to form two-dimensional lattices has hampered efforts to obtain three-dimensional crystals required for X-ray crystallography (12, 31). To our knowledge, only part of the structure of one S-layer protein, SbsC of *Geobacillus stearothermophilus*, has been determined by X-ray crystallography (18). Since high-resolution, three-dimensional structural data are mostly lacking, traditional mutation-based techniques are presently the methods of choice. In cysteine-scanning mutagenesis (CSM), a series of mutant proteins is generated by replacing single residues with cysteine, which contains a sulfhydryl group amenable to further chemical modification. The spatial locations of amino acid residues within the S-layer protein SbsB of gram-positive ther-

* Corresponding author. Mailing address: Department of Basic Veterinary Sciences, Division of Microbiology and Epidemiology, P.O. Box 66, FIN-00014 University of Helsinki, Helsinki, Finland. Phone: 358 9 191 57058. Fax: 358 9 191 57033. E-mail: Airi.Palva@Helsinki.fi.

▽ Published ahead of print on 20 March 2009.

mophile *G. stearothermophilus* PV72/p2 have been analyzed by CSM. A total of 75 residues out of 920 were studied, identifying 23 residues located at the surface of protein monomers, five of those located on the outer surface of the protein lattice (10). These mutant proteins were subsequently analyzed by a cross-linking screen to assess residues accessible in monomeric form to the protein/protein interface and the inner surface of the lattice (12).

In the genus *Lactobacillus*, S-layers have been found in several species. S-layer protein genes have been sequenced from *L. brevis*, *L. helveticus*, and *L. acidophilus* group organisms. Sequence similarity between *Lactobacillus* S-layer protein genes can be found only between closely related *Lactobacillus* species. Therefore, the primary sequences of *Lactobacillus* S-layer proteins show extensive variability, with the number of identical amino acids varying from 7 to 100% between different proteins. As a group, *Lactobacillus* S-layer proteins differ from those of most other bacteria in their smaller sizes (25 to 71 kDa) and higher calculated isoelectric point (pI) values (9.4 to 10.4) (1). The presence of two or more S-layer protein genes in the same strain is common in lactobacilli (5, 6, 11, 28, 35); however, only one S-layer protein gene, *slpA*, has so far been described to be present in the genome of *L. brevis* ATCC 8287. SlpA is a 435-amino-acid, 46-kDa S-layer protein that assembles into a lattice of oblique symmetry on the bacterial surface (2, 36). *L. brevis* ATCC 8287 has GRAS (generally recognized as safe) status and has been shown to possess probiotic properties (21), which make SlpA a very attractive subject, e.g., in the development of live oral vaccines. Moreover, a recent report using differential scanning calorimetry suggests that in comparison with other S-layer proteins, SlpA is resistant to high temperatures (21). This thermal stability could prove potentially useful in a variety of in vitro S-layer applications currently being planned or under development (27, 30, 31). Recently, SlpA was characterized to consist of an N-terminal cell wall binding domain (residues 1 to 178) and a C-terminal self-assembly domain (179 to 435) (3). For the development of applications that take advantage of these characteristics, further investigation of SlpA at the molecular level is essential.

Herein, we use CSM and targeted chemical modification to assign 46 amino acid residues of SlpA to spatial locations in the protein monomer and in the lattice according to their surface accessibility. We focused mainly on the self-assembly domain, the region facing the outer surface of the protein lattice and thus most amenable to insertions and chemical modification. Two different marker molecules were used to modify cysteine-containing mutant proteins that were either in solution or attached to the cell wall. The results were subsequently evaluated taking advantage of the recent new information on SlpA domain boundaries (3). We were able to distinguish residues located in the outer and inner surfaces of the lattice, protein interior, and interface/pore regions. The information gathered here can be used in the development of further biotechnological and nanobiological applications, both in vitro and in vivo, that benefit from a thermostable S-layer protein from a GRAS bacterium with health-beneficial properties.

## MATERIALS AND METHODS

**Bacterial strains and culture conditions.** *Escherichia coli* XL1-Blue supercompetent cells (*recA1 endA1 gyrA96 thi-1 hsdR17 supE44 relA1 lac* [F′ *proAB lacI*$^q$*Z*ΔM15 Tn*10* (Tet$^r$)]) were used in the generation of mutations, and *E. coli* strain BL-21(DE3) [B F$^-$ *dcm ompT hsdS*($r_B^-$ $m_B^-$) *gal* λ(DE3)] was used to express the proteins altered. Both strains were from Stratagene. *E. coli* XL-1 Blue was grown in Luria-Bertani medium, BL-21(DE3) in M9ZB medium (32), and *L. brevis* ATCC 8287 in MRS broth (Difco) at 37°C. When appropriate, kanamycin was used at a concentration of 30 μg/ml.

**Routine DNA manipulations and transformation.** Routine molecular biology techniques were used essentially as described previously (23). Plasmid DNA was isolated using the Wizard Minipreps kit (Promega). The PCR products were purified with the QIAquick PCR purification kit (Qiagen). DNA restriction and modification enzymes were used as recommended by the manufacturers (Stratagene, New England Biolabs). The PCR was carried out with DyNAzyme II DNA polymerase as recommended by the manufacturer (Finnzymes). *E. coli* XL1-Blue supercompetent cells were transformed as recommended by the supplier (Stratagene). BL21(DE3) cells were transformed as described previously (23).

**Oligonucleotides and DNA sequencing.** Oligonucleotides (Oligomer, Helsinki, Finland, and Sigma-Aldrich) used in this work are listed in Table 1. Sequencing of the mutation sites was performed using an ABI Prism 310 genetic analyzer in combination with the DNA sequencing kit for BigDye Terminator cycle sequencing (Applied Biosystems). The sequences of the entire gene constructs were verified by the Sequencing Laboratory of the Institute of Biotechnology, University of Helsinki, Helsinki, Finland.

**Protein analysis.** Protein concentrations were determined by Bio-Rad protein assays (Bio-Rad) using bovine serum albumin as a standard. The protein samples were subjected to sodium dodecyl sulfate-polyacrylamide gel electrophoresis (SDS-PAGE) (14) and stained with Coomassie brilliant blue.

**Construction of SlpA mutant proteins.** Single amino acid mutations were made for 46 amino acid residues (23 threonine, 17 serine, 3 alanine, 2 valine, and 1 leucine) that were dispersed throughout the SlpA amino acid sequence, concentrating on the self-assembly domain defined (3). Site-directed mutagenesis was carried out based on the QuikChange II kit (Stratagene) with the following modifications: as a polymerase, Phusion DNA polymerase (Finnzymes) was used according to the instructions supplied by the manufacturer, and in addition, DpnI digestion was extended to 3 h at 37°C. The PAGE-purified oligonucleotides required were from Sigma-Aldrich. Plasmid pKTH5199 (3), encoding the mature SlpA protein with an N-terminal His tag under a T7 promoter in a pET28a(+) backbone (Novagen) was used as a template in all mutagenesis reactions. The mutations were verified by performing colony PCRs on colonies observed on transformation plates using primers 1568 and 1569, followed by sequencing the resulting PCR products containing the recombinant SlpA gene with primers 622, 1568, and 1569.

**Heterologous expression of sequences encoding SlpA mutant proteins.** Gene expression was carried out using the BL21(DE3) strain as described in the pET system manual (Novagen). Briefly, the expression of SlpA mutant proteins was induced by adding isopropyl-β-D-thiogalactopyranoside (IPTG) at a concentration of 1.0 mM to the medium of exponentially growing *E. coli* strains that harbored an expression plasmid containing the mutation desired. After IPTG was added, the incubation was continued for 5 h. The cells were harvested by centrifugation and the pellets (typically ~1.5 g [wet weight]/200 ml of culture) stored at −80°C until used.

For the purification of mutant proteins, the cells were resuspended in double-distilled water and disrupted with a Branson Sonic Power sonicator (Branson Ultrasonic Corp.), followed by centrifugations for 5 min at 3,000 × *g* and 20 min at 15,000 × *g*. The SlpA mutant proteins were purified from the latter supernatant in the presence of 4 M guanidine hydrochloride (GHCl) with a His Trap HP column according to the instructions given by Amersham Biosciences (binding and washing buffer, 20 mM sodium phosphate, 0.5 M NaCl, 20 mM imidazole [pH 7.4]; elution buffer, same but 0.5 M imidazole). After purification, the fractions containing the SlpA mutant protein were dialyzed overnight at +4°C against a buffer containing 10 mM Tris-HCl (pH 7.5) and 0.1 mM dithiothreitol (DTT). The purity of the proteins isolated was checked by SDS-PAGE.

**Analysis of the lattice formed by wild-type and mutant proteins by EM and small-angle X-ray scattering (SAXS).** Suspensions of all 46 heterologously expressed, isolated, and dialyzed SlpA mutant proteins were examined by negative staining to visualize the self-assembly products by electron microscopy (EM) as described previously (3, 20).

The SAXS measurements were performed using a conventional X-ray tube with $CuK_\alpha$ radiation (wavelength, 1.54 Å). The intensity curves were measured with a HI-STAR area detector at a sample-to-detector distance of 50 cm. The magnitudes of the scattering vector $k$ [$k = (4\pi \sin\theta)/\lambda$, where $2\theta$ is the scattering angle and $\lambda$ is the incident wavelength] were 0.02 to 0.42 $Å^{-1}$ (34). The samples were centrifuged into pellets. The SAXS intensities of the pellets were measured

TABLE 1. Oligonucleotides used in this study[a]

| Oligonucleotide | Sequence (5′–3′) |
|---|---|
| 622* | AACTGATGGTACAAAGGCAGG |
| 1568* | GCTAGTTATTGCTCAGCGG |
| 1569* | TAATACGACTCACTATAGGG |
| T035C | GCTTTATACACGAAGCCAGGTTGTGTTAAGGGTGCTAAG |
| T047C | GGTTGTCGCTTCTAAGGCTTGTATGGCTAAGTTAGCTTC |
| S073C | CACTAACCGTGGTTGCGTTTACTACCGTGTTGTAACGATG |
| T108C | GGTATCAAGTCTGCTGAAACGTGTACTAAGGCTGATATGCC |
| S145C | CAAGGCAAGTAAAGTTTGCCTTTATGGTGTTGCTAAGGAC |
| T174C | CTATCACGTATGTGCTACTAACGGTAGTGGTATTAGTGGTTG |
| S179C | CTATCACGTAACTGCTACTAACGGTTGTGGTATTAGTGG |
| S182C | GCTACTAACGGTAGTGGTATTTGTGGTTGGATTTACGC |
| A187C | GGTTGGATTTACTGTGGTAAGGGCTTCAGTACTACTGC |
| S192C | CTGGTAAGGGCTTCTGTACTACTGCTACTGGTAC |
| T198C | GGCTTCAGTACTACTGCTACTGGTTGCCAAGTACTTGGTGG |
| S205C | GTACACAAGTACTTGGTGGTCTGTGCACTGATAAGTCAG |
| S209C | GGTCTGTCAACTGATAAGTGCGTTACAGCAACCAACG |
| T213C | CTGTCAACTGATAAGTCAGTTACAGCATGCAACGATAACAGTG |
| S232C | CGACTGATGGCACTCAAGTTGGTTGCAACACTTGGG |
| S246C | GGTACAAAGGCAGGTTGTAAGGTAAGCGATAAGGC |
| T256C | CGATAAGGCCGCCGATCAATGTGCTCTTGAAGCC |
| A264C | CTGCTCTTGAAGCCTACATCAATTGTAACAAGCCTAGCG |
| S268C | CTACATCAATGCTAACAAGCCTTGCGGTTACACTG |
| T273C | GCCTAGCGGTTACACTGTATGTAACCCTAATGCTGCAG |
| T281C | CCCTAATGCTGCAGATGCTTGCTATGGTAACACAGTTTAC |
| S291C | GTTTACGCTACTGTTTGCCAAGCAGCTACTTCTAAGG |
| S303C | GGTCGCTTTGAAGGTCTGCGGGACTCCTGTTAC |
| T308C | GGACTCCTGTTTGTACTGCATTGACTACAGCTGATGC |
| T312C | GGACTCCTGTTACTACTGCATTGTGTACAGCTGATGC |
| A316C | CTACTGCATTGACTACAGCTGATTGTAATGATAAGGTTGCAGC |
| V320C | CAGCTGATGCTAATGATAAGTGTGCAGCTAACGATACCAC |
| S330C | CGATACCACTGCTAATGGTTGTTCTGTTGCAGGC |
| S335C | GTAGTTCTGTTGCAGGCTGCACAGTCTATGCTGCTGG |
| T342C | CAACAGTCTATGCTGCTGGTTGTAAGTTGGCTCAATTAACAAC |
| T349C | CTAAGTTGGCTCAATTAACATGTGACTTGACTGGTGAAAAGG |
| V358C | GACTGGTGAAAAGGGTCAATGTGTCACATTAACTGCCATC |
| T362C | GGGTCAAGTTGTCACATTATGTGCCATCGATACTGATTTGG |
| T366C | GTCACATTAACTGCCATCGATTGTGATTTGGAAGACGCTACG |
| T372C | CATCGATACTGATTTGGAAGACGCTTGCTTCACTGGAACTACG |
| T376C | GACGCTACGTTCACTGGATGTACGACTTACTATTCAGATC |
| L383C | GGAACTACGACTTACTATTCAGATTGTGGTAAAGCATACCACTAC |
| T390C | GGTAAAGCATACCACTACTGTTACACTTACAATAAGGACAGTGC |
| S397C | CAATAAGGACTGTGCTGCTTCTTCAAATGCAAGTACCC |
| S400C | CAATAAGGACAGTGCTGCTTGTTCAAATGCAAGTACCC |
| T405C | GTGCTGCTTCTTCAAATGCAAGTTGCCAATTTGGTTCAAACG |
| S409C | GTACCCAATTTGGTTGCAACGTCACTGGTACTTTAACTGCTAC |
| T414C | CAAACGTCACTGGTTGTTTAACTGCTACCCTTGTTATGGG |
| T418C | GTCACTGGTACTTTAACTGCTTGCCTTGTTATGGGTAAGTC |
| S424C | CCCTTGTTATGGGTAAGTGTACTGCTACTGCTAAC |
| T431C | GTAAGTCTACTGCTACTGCTAACGGTTGTACTTGGTTCAAC |

[a] An asterisk denotes a sequencing oligonucleotide. For mutagenesis oligonucleotides, only the forward oligonucleotide is shown; reverse oligonucleotides are reverse complements of the forward sequences shown.

using cell wall fragments without protein as the background pellet. Each sample was measured in 3-h sequences, and one to seven intensity curves were summed together, depending on the sample.

**Solvent accessibility of monomeric mutant proteins.** Monomeric, DTT-free protein solutions were obtained by centrifuging the protein suspensions for 15 min at 16,000 × *g*, washing the protein pellet twice with 10 mM Tris-HCl (pH 7.5), and collecting the last supernatant. These preparations were immediately labeled with maleimide-containing reagents.

The cysteine-containing proteins in monomeric form were modified with branched methyl-capped polyethylene glycol (mPEG)-maleimide TMM$(PEG)_{12}$ (molecular weight [MW] = 2,360.75; Pierce) by using the molecular ratio of 1:100. In a 24-μl reaction mixture, protein was used at the molarity of 1.75 μM, mixed with 175 μM of TMM$(PEG)_{12}$, and incubated at room temperature for 5 min or 1 h. The reaction was stopped by adding *N*-ethyl maleimide (NEM; Sigma-Aldrich) in 60-fold molar excess. The proteins modified were run on SDS-PAGE gels without β-mercaptoethanol. The bands were visualized with Coomassie blue R-250 stain (Santa Cruz Biotechnology) and analyzed using Alpha Ease FC (Alpha Innotech) or AIDA image analyzer (Raytest) software.

The cysteine-containing proteins in monomeric form were modified with AlexaFluor488 $C_5$-maleimide (MW = 720.66; Molecular Probes) using the molecular ratio of 1:1. In a 48-μl reaction mixture, each protein was used at a molarity of 1.75 μM and the reaction mixture was incubated on ice for 10 s, 30 s, or 120 s. The reaction was stopped by adding NEM in 600-fold molar excess. The proteins modified were run on SDS-PAGE gels without β-mercaptoethanol. The bands were visualized using the FLA-5100 imaging system with FLA Fluor Stage 4046 tray and 473-nm laser (Fujifilm) and analyzed with AIDA Image Analyzer software.

**Solvent accessibility of cell wall-bound mutant proteins.** Isolated cell wall fragments of *L. brevis* ATCC 8287 and the cell wall-bound protein preparations were obtained as described previously (3). The cell wall-bound cysteine-containing proteins were modified with TMM$(PEG)_{12}$ using the calculated amount of 2 μg of each mutant protein on the cell wall fragments and the molecular ratio of

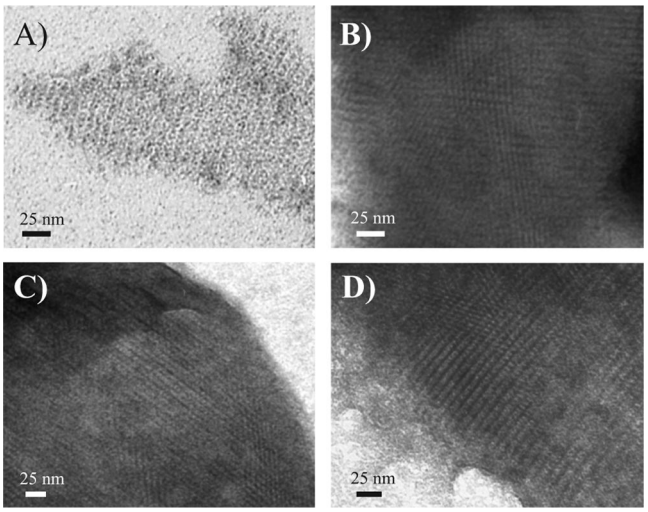


FIG. 1. Electron micrographs of negative-stained self-assembly products of heterologously expressed, His-tagged nonmutated SlpA (A) and SlpA mutant proteins S182C (B), S232C (C), and A264C (D) show the same type of oblique lattice.

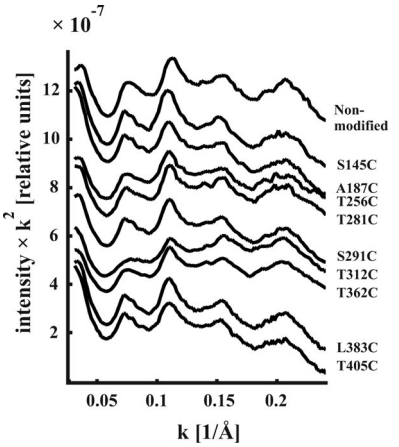


FIG. 2. Small-angle X-ray scattering intensities of SlpA cysteine mutant proteins on the *Lactobacillus brevis* cell wall fragments. The curves from top to bottom: nonmutated SlpA and S145C, A187C, T256C, T281C, S291C, T312C, T362C, L383C, and T405C mutant proteins.

1:100 [protein/TMM(PEG)$_{12}$] in the total reaction mixture volume of 16 μl. The reaction mixtures were incubated for 1, 3, or 5 min at room temperature and stopped by NEM as described above, and the modified proteins were analyzed by SDS-PAGE as described for the monomeric proteins.

**Analysis of primary amino acid sequences.** The predictions of the cleavage sites of trypsin were obtained using the PeptideCutter program of the ExPASy server (http://au.expasy.org/tools/peptidecutter) (9). The predictions of secondary structure and surface accessibility, as well as the pI value, were obtained using the PredictProtein program (www.predictprotein.org) (22). In addition, SA BLE (http://sable.cchmc.org) and JNET (www.compbio.dundee.ac.uk/~www-jpred) predictions of surface accessibility were compared with the results obtained in this work.

## RESULTS

**Construction of mutant proteins.** We generated a series of 46 mutant proteins of the *L. brevis* ATCC 8287 S-layer protein SlpA in which a single amino acid residue was changed into a cysteine. All the mutant proteins were derived from a mature wild-type 435-amino-acid SlpA lacking the signal peptide but containing an N-terminal His-tag sequence.

All the mutant proteins were generated by site-directed, PCR-based mutagenesis and were verified by DNA sequencing. We targeted mostly serine and threonine, polar residues often concentrated on the surface of proteins (15, 33) and abundant in the SlpA protein sequence. In addition, the conservative replacement of serine or threonine with cysteine is likely to cause minimal changes to the protein self-assembly process (10). Of the 46 mutant proteins generated, all contained only the single residue substitution desired in their coding region, except for one mutant (S246C) protein, which contained an additional spontaneous, but benign, point mutation (T348A).

The proteins were produced using IPTG induction in the *E. coli* BL21(DE3) expression strain and purified by affinity chromatography using His-tag columns. The average protein yield from a 200-ml culture was ~5 mg, and the purity of the mutant proteins was verified by SDS-PAGE. Under reducing conditions (β-mercaptoethanol or DTT), the migration pattern of all the mutant proteins was identical to that of wild-type SlpA, corresponding to a 46-kDa protein. In the absence of reducing agents, an additional minor band of ~100 kDa was observed in all the mutant protein samples and likely represented a dimeric protein formed through the cysteine sulfhydryl groups.

**Analysis of the lattice formed by the wild-type and mutant proteins by EM and SAXS.** To test whether the SlpA mutant proteins had the capacity to form self-assembly products, denatured proteins were dialyzed and the resulting precipitates were analyzed by negative staining and EM. A regular pattern of oblique lattice symmetry essentially identical to that formed by nonmutated SlpA (Fig. 1A) was detected for all the SlpA mutant proteins. Examples of such lattice formation are shown in Fig. 1B, C, and D.

The ability of nonmutated SlpA to form lattice on cell wall fragments has been examined by cryo-EM and SAXS analysis (P. Jääskeläinen et al., unpublished data). To validate the ability of SlpA mutant proteins to form lattice in a similar manner, selected SlpA mutants were analyzed with SAXS, the results of which are summarized in Fig. 2. All SAXS intensity curves showed indistinguishable diffraction maxima, indicating that all of the mutant proteins examined displayed crystal properties essentially identical to those of the nonmutated SlpA.

**Solvent accessibility of monomeric mutant proteins.** To assess the surface accessibility of the residues altered by cysteine substitution, the SlpA mutant proteins were subjected to sulfhydryl-specific modification as monomeric proteins in an aqueous solution. Two differing modification systems were used: a branched mPEG-maleimide reagent, TMM(PEG)$_{12}$, with a molecular mass of ~2.4 kDa and a smaller labeling reagent, Alexa-Fluor488-maleimide, with a molecular mass of 0.7 kDa. Both markers are hydrophilic, making them more likely to react with residues localized on the outer surface of the protein.

The extent to which the monomeric proteins were modified by labeling with TMM(PEG)$_{12}$ was monitored at the 5-min and 1-h time points by SDS-PAGE (Fig. 3, PEG-mono), and the TMM(PEG)$_{12}$-modified SlpA proteins (~48.5 kDa) were distinguished from nonmodified proteins (46 kDa) by differential

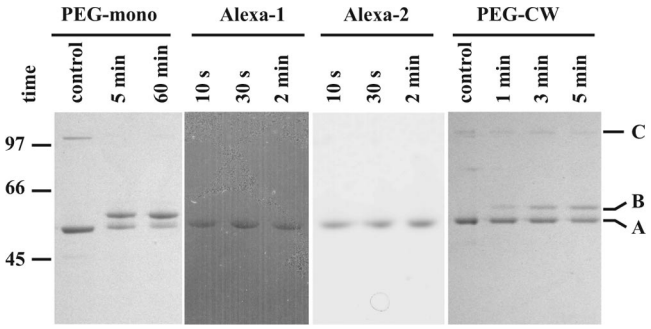


FIG. 3. Examination of the surface accessibility of cysteine sulfhydryl groups of SlpA monomers in solution and proteins assembled on cell wall fragments using a gel shift assay. PEG-maleimide modification of proteins as monomers (PEG-mono) and assembled on cell wall fragments (PEG-CW) yield a band migrating slower (B) than nonmodified SlpA (A) on an SDS-PAGE gel. Modification with Alexa-Fluor488-maleimide yields a band that is not distinguishable from that of a nonmodified protein by migration. However, modified protein can be visualized with a fluorescent filter (Alexa-1) and the band can be compared with the protein band visualized with Coomassie stain (Alexa-2). A minor band corresponding to the protein dimer (C) is visible especially in nonmodified samples. The bands of mutant T366C are shown here as an example.

migration. The results of the 5-min reaction are summarized in Fig. 4A and generally indicated that the modification reaction was rapid. In 11 of the 46 mutant proteins studied, more than 75% of the protein molecules were already modified after 5 min of incubation. However, the differences in the speed and extent of modification between individual mutant proteins were noticeable, e.g., eight mutant proteins were less than 25% modified after 5 min of incubation. The amount of modification also varied notably between mutant proteins with cysteine residues located close to each other in the primary amino acid sequence (e.g., mutant proteins T273C/T281C, A316C/V320C, and T372C/T376C). After 1 h of incubation, the differences between mutant proteins were less pronounced, as 42 of 46 mutant proteins were at least 50% modified. However, two mutant proteins, T281C and V320C, remained less than 25% modified even after 1 h.

Monomeric proteins labeled with AlexaFluor488-maleimide for 10, 30, or 120 s were analyzed by SDS-PAGE and visualized under 473-nm light with a fluorescent filter. Fluorescence signal levels were compared with protein concentrations determined by Coomassie staining of the same gels (Fig. 3, Alexa-1 and Alexa-2, respectively). Due to a much higher reaction rate with AlexaFluor488-maleimide than with the larger PEG-maleimide, several proteins reached their maximal modification state in 10 s, and after 30 s, further modification was negligible. The results of the 30-s reaction are shown in Fig. 4B. Compared with PEG-maleimide, the modification of cysteine residues with AlexaFluor488-maleimide was generally either very strong or almost minimal. The difference between the residues located close to each other (e.g., T308C/T312C and V358C/T362C) was even more pronounced when modified with AlexaFluor488. Still, the most extensively modified residues were the same using both modifying reagents, as were the least modified residues. Taking the two experiments together, 24 of the 46 (52%) mutant proteins tested had cysteine residues that were highly accessible (on average, modified >67% of the most modified residue), while 10 (22%) were moderately accessible (modified 33 to 67% of the most-modified residue) and 11 (24%) were poorly accessible (modified <33% of the most-modified residue). One mutant (T281C) had a cysteine residue that was classified as totally inaccessible in the conditions used.

**Solvent accessibility of cell wall-bound mutant proteins.** To determine the surface accessibility of the proteins attached to the cell wall, mutant SlpA proteins assembled on the surfaces of isolated cell wall fragments of *L. brevis* were modified with PEG-maleimide. The labeling reactions (1, 3, or 5 min) were carried out with molecular ratios similar to that for the monomeric protein experiment and analyzed by SDS-PAGE (Fig. 3, PEG-CW). All of the mutant proteins were still in the linear range of modification between the 3- and 5-min time points.

A summary of the results of the 5-min reaction is shown in Fig. 4C. Overall, 9 mutant proteins (20%), all with residues classified as highly accessible in the monomer experiment, had residues regarded as very accessible (modified at least 50% of the most-modified residue), while 7 (15%) were moderately accessible (modified 20 to 50% of the most-modified residue), 7 (15%) poorly accessible (modified 0.1 to 20% of the most-modified residue), and 23 mutant proteins (50%) had residues that were entirely inaccessible in the conditions used. Repeated experiments on mutant proteins with very accessible residues yielded practically identical results, indicating very good reproducibility.

Figure 5 depicts the comparison of the mutant proteins modified with the three different labeling reactions. Overall, the results from the three labeling reactions correlate with one another. The self-assembly domain of SlpA can be divided into different segments of approximately 20 to 30 amino acids based on their accessibility. These segments have fairly well-defined boundaries, as indicated by the fact that in several cases residues located close to each other can have very different values of accessibility (e.g., A316C/V320C and T372C/T376C).

All 12 residues that were poorly accessible in protein monomers were also poorly accessible in cell wall-bound proteins, indicating a location in the protein interior. Contrastingly, the residues most accessible to modification in the cell wall-bound SlpA clustered into four segments located in the middle of the self-assembly domain: residues 256 to 273, 303 to 316, 335 to 349, and 362 to 372. Notably, a cluster between residues 400 to 414, while accessible in the monomer, was poorly accessible in the cell wall-bound SlpA.

Nine mutated residues that are located in the cell wall-binding domain (1 to 178) were highly or moderately accessible in the monomeric SlpA but almost completely inaccessible in the cell wall-bound protein. In addition, residues located at the N-terminal end (S179C, S182C, and A187C) of the self-assembly domain (179 to 435) shared the same pattern of accessibility, suggesting that in the protein lattice, these residues are located in the inner surface of the S-layer lattice facing the cell wall. Located deeper within the self-assembly domain, residues S192C, T198C, S205, S209, and T213C also showed remarkably lower accessibility as cell wall-bound protein than as monomeric proteins. Moreover, several other residues (S232, T273C, S291C, S400C, T405C, and S409C) displayed a prominent decrease in

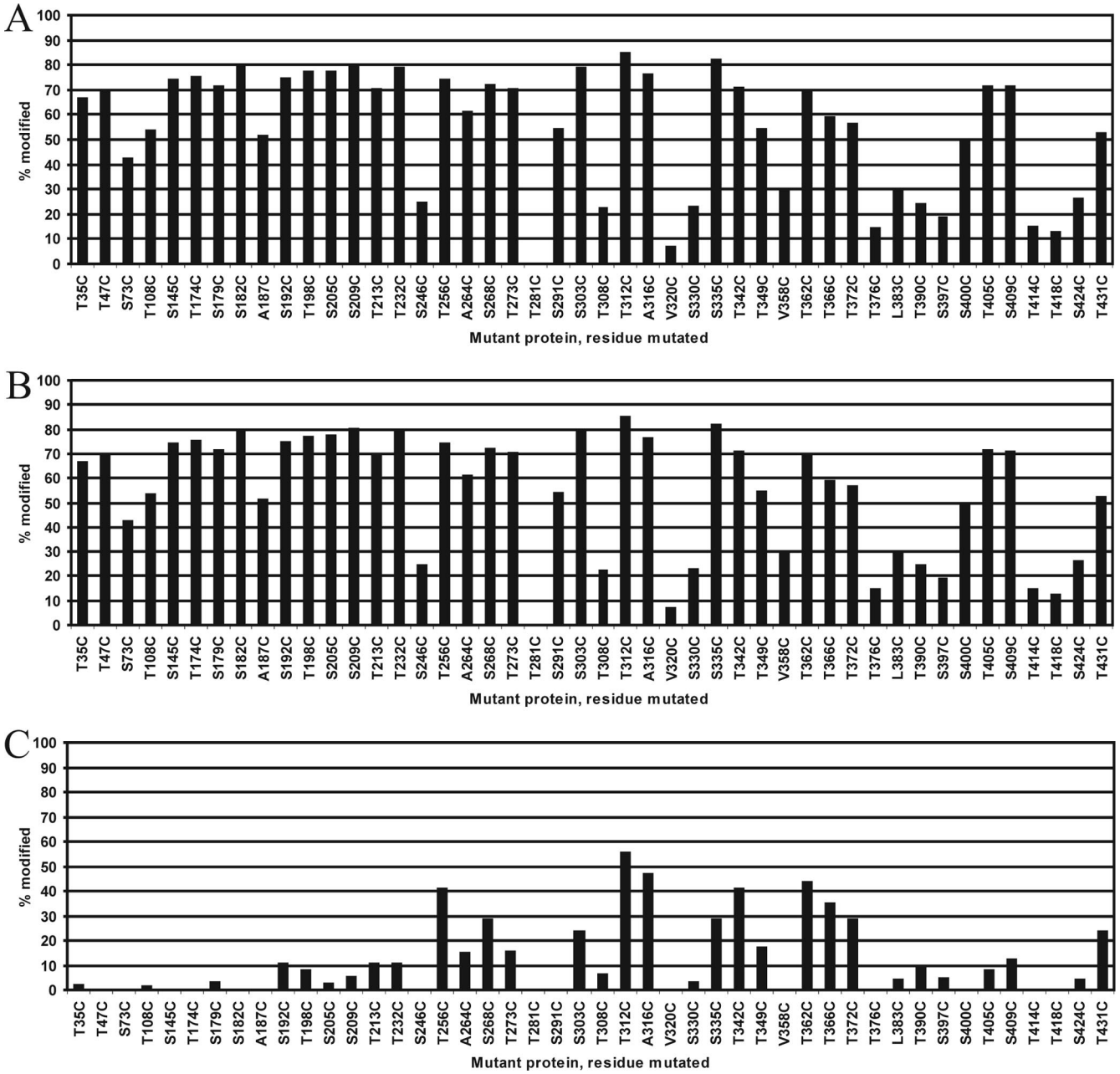


FIG. 4. Accessibility of the sulfhydryl group of cysteine in the SlpA mutant proteins modified. Monomeric proteins in solution modified with PEG-maleimide for the 5-min reaction (A) and AlexaFluor488-maleimide for the 30-s reaction (B). (C) Proteins assembled on cell wall fragments modified with PEG-maleimide (5-min reaction). Bars indicate the proportion of modified protein from total protein (A and C) or the intensity of the fluorescence marker signal compared with the highest signal observed (B).

accessibility from monomeric to cell wall-bound protein, suggesting their localization at the protein-protein interface.

## DISCUSSION

To better understand the molecular structure of the *L. brevis* S-layer protein SlpA and the roles of individual amino acid residues within the structure, we generated a series of proteins in which a single amino acid residue was replaced with cysteine. All 46 mutant proteins generated were able to form self-assembly products in an aqueous solution, indicating that mutations introduced do not markedly affect the conformation of SlpA. In contrast, a similar study of *G. stearothermophilus* S-layer protein SbsB reported that three of 75 mutant proteins showed reduced ability to form regular lattices. However, due to random PCR errors and a restriction enzyme-dependent screening method, all SbsB mutant proteins contained another amino acid change adjacent to the cysteine, possibly affecting their lattice-forming properties (10).

The high number of surface-accessible residues in monomeric

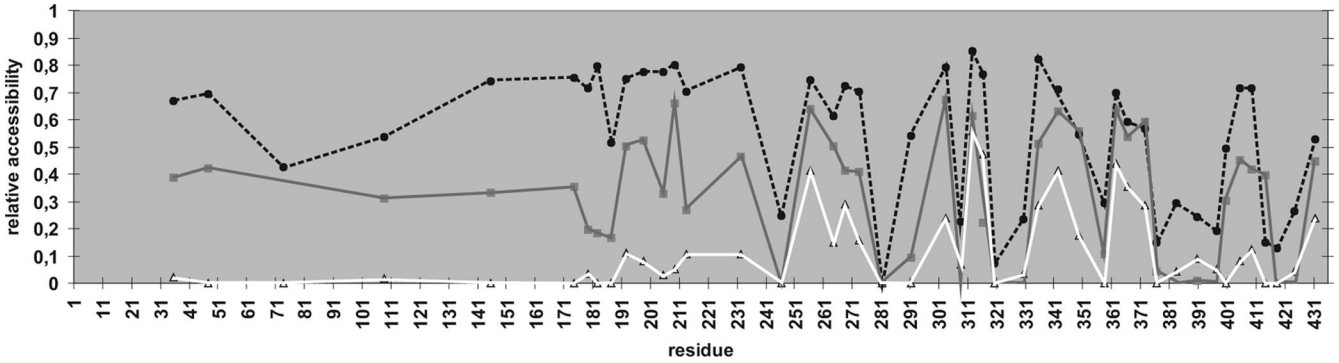


FIG. 5. Comparison of the surface accessibility of mutated amino acid residues modified. Relative accessibility is given as a value between 0 and 1 and denotes the proportion of protein that is modified after 5 min (PEG-maleimide) or 30 s (AlexaFluor488-maleimide) of reaction from the total protein. The solvent accessibility of cysteine residues in protein monomers is shown as dotted black (PEG-maleimide) and solid gray (AlexaFluor488-maleimide) lines. The accessibility of residues in cell wall-bound proteins modified with PEG-maleimide is shown as a white line.

protein is in accordance with results derived from *G. stearothermophilus* SbsB (10). All of the residues that were almost or totally inaccessible in the monomeric form were found within the C-terminal half of the protein, suggesting that these residues are located inside a structurally compact region of the self-assembly domain. This finding is consistent with a previous trypsin cleavage experiment (3), which identified a trypsin-resistant region encompassing residues (190) 209 to 423 (see below).

The ability of the recombinant SlpA protein to self-assemble in dialysis as a lattice on isolated cell wall fragments has been shown using cryo-EM and SAXS (Jääskeläinen et al., unpublished). As was confirmed by SAXS analysis, crystals of mutated proteins that are attached to cell wall fragments are similar to those formed by nonmutated SlpA. Thus, the surface accessibility of mutated residues within a lattice structure could be analyzed. In general, the observed accessibility of all the mutated residues was lower when attached to the cell wall than as monomers in solution. The differences in reaction kinetics and the more constrained structure of the lattice compared with the protein monomer in solution obviously contribute to the reduced level of accessibility observed. Additional reasons for this phenomenon include obstruction of the inner surface of the protein lattice by the cell wall, as well as part of the monomer surface being shielded at the subunit-subunit interface of the lattice or obstructed in lattice pores (10, 12).

As evidenced by the inaccessibility of the residues located in the cell wall-binding domain (residues 1 to 178) while SlpA is attached to a cell wall fragment, $TMM(PEG)_{12}$ is not able to permeate the cell wall and gain access to the cysteine residues in the conditions used. This is feasible since, assuming that it has a spherical shape, a 2.5-kDa PEG polymer has a hydrodynamic diameter of approximately 3.0 nm (26), which is significantly smaller than the 5.2 nm of a 5-kDa PEG used with *G. stearothermophilus* (10) but between the exclusion limits of isolated cells walls from *Bacillus megaterium* (2.2 nm) (26) and *Bacillus subtilis* (4.2 nm) (7). Based on the hydrodynamic diameter, it can be assumed that a 2.5-kDa PEG occupies an area of $\sim 9$ nm$^2$. Compared to the lattice constants of SlpA ($a = 10.38$ nm, $b = 6.36$ nm, 72.7° for nonmutated protein) (3), it is likely that only the residues facing the largest pores of the lattice are accessible to $TMM(PEG)_{12}$.

Based on the accessibility data, the mutated residues can be divided into four groups (Table 2) according to different locations within the protein lattice. (i) Residues inaccessible to modification even in the monomeric form of the protein (modified less than 30% of the most-modified residue) are likely located within the interior of the protein. (ii) Residues that are highly accessible in both monomeric and cell wall-bound forms of the protein (modified more than 50% of the most-modified residue in the cell wall-bound form) are likely located on the outer surface of the protein lattice. (iii) Residues located in the cell wall-binding domain (1 to 178) that showed medium to high accessibility in the monomer experiment yet had only poor accessibility while the protein was bound to the cell wall are likely located on the inner surface of the protein lattice. In addition, this assignment likely applies to residues located in the immediate N-terminal end of the self-assembly domain (S179C, S182C, and T187C). (iv) Residues located further into the self-assembly domain showed markedly better accessibility in the monomer experiment than when the protein was bound to the cell wall. In this fourth group, the residues could be located in the protein-protein interface between subunits, flanking the pores of the S-layer lattice, or possibly in the inner surface of the lattice facing the cell wall.

We also analyzed the sequences surrounding the mutated residues in a seven-amino-acid window (Table 2). Each group, formed on the basis of experimental results, has a distinct profile of amino acid composition, thus supporting the assignments made. Notably, the amount of hydrophobic (nonpolar) amino acids is fairly constant (42 to 46% of the residues) in all the groups. While contradictory to the results derived from *G. stearothermophilus* SbsB (12), this is not surprising given that in general hydrophobic residues are evenly spread throughout the SlpA amino acid sequence, as evidenced by a hydropathy plot which reveals no extensive hydrophobic or hydrophilic regions (data not shown). However, there are remarkable differences between the groups in the amounts of polar and charged amino acids, as well as in the net charge of the seven-amino-acid sequences.

On average, the sequences around residues mapped to the protein interior have 14% of charged residues and similar amounts of polar and hydrophobic residues (43% each). The net charge is slightly positive (+0.33). As can be expected, the residues mapped to the outer surface of the lattice are in a

TABLE 2. Mutant proteins generated grouped according to their accessibility and the amino acid compositions of insertion sites using seven-amino-acid windows

| Location and mutant no. | Sequence[a] | No. of charged amino acids | No. of polar amino acids | No. of nonpolar amino acids | Net charge | % Charged residues | % Polar residues | % Nonpolar residues |
|---|---|---|---|---|---|---|---|---|
| Interior ($n$ = 12) | | | | | | | | |
| 246 | KAG**S**KVS | 2 | 2 | 3 | +2 | 28.6 | 28.6 | 42.9 |
| 281 | ADA**T**YGN | 1 | 3 | 3 | −1 | 14.3 | 42.9 | 42.9 |
| 308 | TPV**T**TAL | 0 | 3 | 4 | 0 | 0.0 | 42.9 | 57.1 |
| 320 | NDK**V**AAN | 2 | 2 | 3 | 0 | 28.6 | 28.6 | 42.9 |
| 330 | ANG**S**SVA | 0 | 3 | 4 | 0 | 0.0 | 42.9 | 57.1 |
| 358 | KGQ**V**VTL | 1 | 2 | 4 | +1 | 14.3 | 28.6 | 57.1 |
| 376 | FTG**T**TTY | 0 | 5 | 2 | 0 | 0.0 | 71.4 | 28.6 |
| 383 | YSD**L**GKA | 2 | 2 | 3 | 0 | 28.6 | 28.6 | 42.9 |
| 390 | YHY**T**YTY | 1 | 6 | 0 | +1 | 14.3 | 85.7 | 0.0 |
| 397 | NKD**S**AAS | 2 | 3 | 2 | 0 | 28.6 | 42.9 | 28.6 |
| 418 | LTA**T**LVM | 0 | 2 | 5 | 0 | 0.0 | 28.6 | 71.4 |
| 424 | MGK**S**TAT | 1 | 3 | 3 | +1 | 14.3 | 42.9 | 42.9 |
| Avg | | | | | +0.33 | 14.3 | 42.9 | 42.9 |
| Interface/pore ($n$ = 16) | | | | | | | | |
| 192[b] | KGF**S**TTA | 1 | 3 | 3 | +1 | 14.3 | 42.9 | 42.9 |
| 198[b] | ATG**T**QVL | 0 | 3 | 4 | 0 | 0.0 | 42.9 | 57.1 |
| 205[b] | GGL**S**TDK | 2 | 2 | 3 | 0 | 28.6 | 28.6 | 42.9 |
| 209[b] | TDK**S**VTA | 2 | 3 | 2 | 0 | 28.6 | 42.9 | 28.6 |
| 213[b] | VTA**T**NDN | 1 | 4 | 2 | −1 | 14.3 | 57.1 | 28.6 |
| 232[b] | QVG**S**NTW | 0 | 5 | 2 | 0 | 0.0 | 71.4 | 28.6 |
| 264[c] | YIN**A**NKP | 1 | 3 | 3 | +1 | 14.3 | 42.9 | 42.9 |
| 273[b] | YTV**T**NPN | 0 | 5 | 2 | 0 | 0.0 | 71.4 | 28.6 |
| 291[b] | ATV**S**QAA | 0 | 3 | 4 | 0 | 0.0 | 42.9 | 57.1 |
| 303[c] | LKV**S**GTP | 1 | 2 | 4 | +1 | 14.3 | 28.6 | 57.1 |
| 349[c] | QLT**T**DLT | 1 | 4 | 2 | −1 | 14.3 | 57.1 | 28.6 |
| 400[b] | SAA**S**SNA | 0 | 4 | 3 | 0 | 0.0 | 57.1 | 42.9 |
| 405[b] | NAS**T**QFG | 0 | 4 | 3 | 0 | 0.0 | 57.1 | 42.9 |
| 409[b] | QFG**S**NVT | 0 | 4 | 3 | 0 | 0.0 | 57.1 | 42.9 |
| 414[c] | VTG**T**LTA | 0 | 3 | 4 | 0 | 0.0 | 42.9 | 57.1 |
| 431[c] | ANG**T**TWF | 0 | 4 | 3 | 0 | 0.0 | 57.1 | 42.9 |
| Avg | | | | | +0.06 | 8.0 | 50.0 | 42.0 |
| Outer surface ($n$ = 9) | | | | | | | | |
| 256 | ADQ**T**ALE | 2 | 2 | 3 | −2 | 28.6 | 28.6 | 42.9 |
| 268 | NKP**S**GYT | 1 | 4 | 2 | +1 | 14.3 | 57.1 | 28.6 |
| 312 | TAL**T**TAD | 1 | 3 | 3 | −1 | 14.3 | 42.9 | 42.9 |
| 316 | TAD**A**NDK | 3 | 2 | 2 | −1 | 42.9 | 28.6 | 28.6 |
| 335 | VAG**S**TVY | 0 | 3 | 4 | 0 | 0.0 | 42.9 | 57.1 |
| 342 | AAG**T**KLA | 1 | 1 | 5 | +1 | 14.3 | 14.3 | 71.4 |
| 362 | VTL**T**AID | 1 | 2 | 4 | −1 | 14.3 | 28.6 | 57.1 |
| 366 | AID**T**DLE | 3 | 1 | 3 | −3 | 42.9 | 14.3 | 42.9 |
| 372 | EDA**T**FTG | 2 | 2 | 3 | −2 | 28.6 | 28.6 | 42.9 |
| Avg | | | | | −0.89 | 22.2 | 31.7 | 46.0 |
| Inner surface ($n$ = 9) | | | | | | | | |
| 35 | KPG**T**VKG | 2 | 1 | 4 | +2 | 28.6 | 14.3 | 57.1 |
| 47 | SKA**T**MAK | 2 | 2 | 3 | +2 | 28.6 | 28.6 | 42.9 |
| 73 | NRG**S**VYY | 1 | 4 | 2 | +1 | 14.3 | 57.1 | 28.6 |
| 108 | AET**T**TKA | 2 | 3 | 2 | 0 | 28.6 | 42.9 | 28.6 |
| 145 | SKV**S**LYG | 1 | 3 | 3 | +1 | 14.3 | 42.9 | 42.9 |
| 174 | YHV**T**ATN | 1 | 4 | 2 | +1 | 14.3 | 57.1 | 28.6 |
| 179 | TNG**S**GIS | 0 | 4 | 3 | 0 | 0.0 | 57.1 | 42.9 |
| 182 | SGI**S**GWI | 0 | 3 | 4 | 0 | 0.0 | 42.9 | 57.1 |
| 187 | WIY**A**GKG | 1 | 2 | 4 | +1 | 14.3 | 28.6 | 57.1 |
| Avg | | | | | +0.89 | 15.9 | 41.3 | 42.9 |
| Full-length SlpA | | | | | | 17.5 | 41.6 | 40.9 |
| Self-assembly domain | | | | | | 14.0 | 44.7 | 41.3 |

[a] Mutated residues are in bold.
[b] Putative interface.
[c] Putative pore.

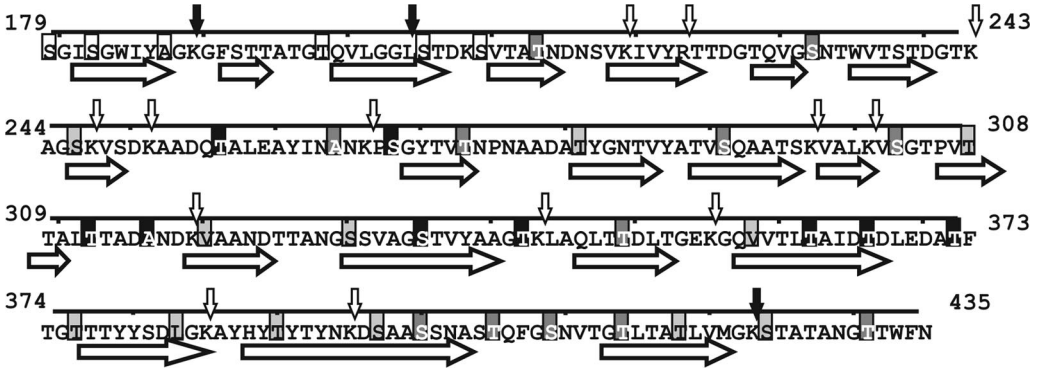


FIG. 6. Solvent accessibility of mutated residues in the self-assembly domain of SlpA compared with PredictProtein predictions of secondary structure (horizontal block arrows indicate β-strands). Mutated residues are shaded according to their assignment: black, outer surface; medium gray, pore/interface; light gray, protein interior; and white, inner surface. Observed and additional predicted (PeptideCutter) cleavage sites of trypsin are marked with small vertical arrows in black and white, respectively.

more hydrophilic and charged (22% of the residues) environment with a negative net charge (−0.89 on average). These results are in accordance with those for SbsB, in which the residues assigned to the outer surface have an average net charge of −1.75 and 39% of the residues within the window are charged (12). Interestingly, the self-assembly domain (residues 179 to 435) of SlpA has a low calculated pI of 5.04.

Also in agreement with the results from the SbsB study (12), residues mapped to the inner surface of the lattice (from the N terminus up to T187C) share a similar, positively charged (SlpA, +0.89, and SbsB, +0.3, on average) amino acid composition. This suggests that SlpA S-layers could be assembled on a negatively charged support. Contrastingly, the surrounding environment of the residues in the interface/pore group appears to be almost totally devoid of charge with an average net charge of +0.06 and 7.6% charged residues. These numbers are notably different from the interface residues of SbsB (+0.5 net charge, 29% charged residues). However, with SbsB only four such residues were detected, limiting the statistical value of average composition (12).

Finally, the interface/pore group could be divided further into distinct subgroups. The difference in accessibility between monomeric and cell wall-bound protein is likely to be more substantial with the residues located at the interface than with residues flanking the pores of the lattice or located within the depressed areas on the protein surface. In addition, residues situated in the depressions of the protein surface are likely to be relatively more reactive toward the smaller AlexaFluor488-maleimide marker than the larger-sized $TMM(PEG)_{12}$. According to these two criteria, the residues could be divided further into the putative interface and pore subgroups shown in Table 2. For further characterization of these residues, a cross-link assay detecting residues located in the protein-protein interface (12) could be conducted in a future study.

A previous study on SlpA used a hydrophilicity profile to predict suitable, exposed insertion sites from the primary protein sequence, and introduced an 11-amino-acid VP1 epitope at positions A49/K50, K251/A252, A316/N317, and D365/T366. Of these sites, only K251/A252 and D365/T366 yielded an antibody response (2). In contrast, our results suggest that A316C and T366C are among the most accessible residues studied. This discrepancy is probably due to either aberration of the protein structure caused by the peptide insert or the difference in the interactions involved in an epitope-antibody binding compared with a sulfhydryl group-maleimide reaction.

The SlpA protein is known to contain two trypsin-resistant fragments, encompassing amino acids 190 to 423 and 209 to 423, suggesting the existence of a compact domain structure between these residues (3). In addition, there are 13 other potential cleavage sites located within the self-assembly domain of SlpA (Fig. 6). One of these sites is situated next to a residue mutated in our study (V320C) that remains almost completely nonmodified in monomeric protein, indicating a buried location deep inside a compact protein structure. Nine other cleavage sites are located close to or in between residues assigned to either the interior or interface/pore, presumably inaccessible to trypsin. However, two putative cleavage sites (residues 266 and 343) are located within the window of residues assigned to the outer surface of the protein and another (residue 251) at an evidently accessible VP1 insertion site, K251/A252 (2). These results reinforce the fact that surface accessibility can be measured with several different methods and that the accessibility of a sulfhydryl group of a given residue to a small maleimide derivative does not always correlate with the accessibility of a nearby peptide bond to a much larger trypsin molecule (MW = 24,000). Interestingly, mutated residue S424C is only poorly accessible in a protein monomer despite being situated next to the functional trypsin cleavage site at 423. The reason for this discrepancy might be the difference in molecular concentrations used, the reaction time, or the higher reaction temperature used with trypsin. A cleavage site close to the unanchored C terminus of the protein could be made accessible simply by increased thermal motion at 37°C.

The prediction of the secondary and tertiary structures of S-layer proteins with algorithms developed with other types of proteins has been difficult. With SlpA, different programs and settings typically yield vastly different types of secondary structure predictions. However, a recent Fourier transform infrared spectroscopy study of SlpA estimated that the protein consists of 0% α-helix, 50.2% β-strand, and 49.8% β-turn and nonordered structures (16). Reasonably well in accordance with these results, PredictProtein (22) estimates for the whole pro-

tein were 0% α-helix, 59.1% β-strand, and 40.9% loop, i.e., other structures. Figure 6 depicts a projection of the mutant assignments made with the secondary structure of the self-assembly domain of SlpA predicted from the amino acid sequence by PredictProtein. Overall, the assignments made in our study are in agreement with the secondary structure predictions. Excluding S335C, T362C, and T366C, residues assigned to the outer surface of the lattice are located in the predicted loops. In contrast, with the exception of T376C and S424C, residues assigned to the protein interior are located within the predicted β-strands. Residues assigned to interface/pore are located within both loops and β-strands predicted. Furthermore, as the prevalence of the β-strand with PredictProtein is higher than the actual observed prevalence of β-strands, it is possible that the β-strands predicted to cover residues 330 to 340 and 357 to 367, spanning residues assigned to the outer surface, are shorter than predicted or do not exist in the actual protein.

In contrast to secondary structure, the prediction of solvent accessibility from the amino acid sequence by PredictProtein poorly matches the results obtained in our cysteine-labeling mutant study. The solvent accessibility predictions of other programs tested (SABLE and JNET) were even worse at reflecting the experimental results obtained (data not shown), further confirming that prediction programs are presently unable to accurately predict the solvent accessibility profile for SlpA or, presumably, other S-layer proteins. In the absence of three-dimensional crystals required for structural determination by X-ray crystallography, CSM remains one of the most reliable methods for assessing the surface accessibility of individual amino acid residues. Furthermore, preliminary studies on live bacteria indicate that epitopes inserted into residues of similar surface accessibility can yield markedly different antibody responses (S. Åvall-Jääskeläinen, personal communication). This phenomenon may be caused by the spatial constraints of the inserted epitope or the effect of the epitope on the refolding of the protein on the bacterial surface. Thus, the identification of several surface-accessible residues—and putative insertion sites—is crucial for potential future applications that utilize live bacteria.

Our results, gained from 46 single-cysteine mutant proteins of SlpA, further confirm the two-domain model of the protein. In addition, we were able to classify the mutated residues according to their solvent accessibility into four different groups: outer surface, pores/protein interface, inner surface of the lattice, and protein interior. The amino acid compositions around mutated residues as well as the predicted secondary structure support the assignments made based on observed accessibility. These results can be used to develop an accurate model for S-protein structure prediction. The residues placed on the outer surface have practical value in potential further applications, e.g., the surface display of effector molecules. In addition, the residues located at the outer surface could be further modified, e.g., to immobilize bacterial cells to solid support. Moreover, the residues located at the protein-protein interface could be further examined to elucidate the interactions involved in the formation of a two-dimensional lattice.

## ACKNOWLEDGMENTS

This work was supported by the EU FP6 EC-STREP project NASSAP 13523. In addition, the University of Helsinki has supported this work with funding aimed at education and research on nanotechnology. The work was performed in the Centre of Excellence on Microbial Food Safety Research, Academy of Finland.

We thank Ilkka Palva for valuable discussions and critical reading of the manuscript. Esa Pohjolainen, Katariina Kojo, and Outi Immonen are thanked for skillful technical assistance. Peter Engelhart is thanked for advice with SAXS sample preparation and Ritva Serimaa for advice with the interpretation of the SAXS results. Silja Åvall-Jääskeläinen is thanked for critical reading of the manuscript. Ingemar von Ossowski is thanked for helpful advice with scientific English.

## REFERENCES

1. **Avall-Jaaskelainen, S., and A. Palva.** 2005. *Lactobacillus* surface layers and their applications. FEMS Microbiol. Rev. **29:**511–529.
2. **Avall-Jaaskelainen, S., K. Kyla-Nikkila, M. Kahala, T. Miikkulainen-Lahti, and A. Palva.** 2002. Surface display of foreign epitopes on the *Lactobacillus brevis* S-layer. Appl. Environ. Microbiol. **68:**5943–5951.
3. **Avall-Jaaskelainen, S., U. Hynonen, N. Ilk, D. Pum, U. B. Sleytr, and A. Palva.** 2008. Identification and characterization of domains responsible for self-assembly and cell wall binding of the surface layer protein of *Lactobacillus brevis* ATCC 8287. BMC Microbiol. **8:**165.
4. **Blaser, M. J., E. Wang, M. K. Tummuru, R. Washburn, S. Fujimoto, and A. Labigne.** 1994. High-frequency S-layer protein variation in *Campylobacter fetus* revealed by *sapA* mutagenesis. Mol. Microbiol. **14:**453–462.
5. **Boot, H. J., C. P. Kolen, and P. H. Pouwels.** 1995. Identification, cloning, and nucleotide sequence of a silent S-layer protein gene of *Lactobacillus acidophilus* ATCC 4356 which has extensive similarity with the S-layer protein gene of this species. J. Bacteriol. **177:**7222–7230.
6. **Boot, H. J., C. P. Kolen, B. Pot, K. Kersters, and P. H. Pouwels.** 1996. The presence of two S-layer-protein-encoding genes is conserved among species related to *Lactobacillus acidophilus*. Microbiology **142:**2375–2384.
7. **Demchick, P., and A. L. Koch.** 1996. The permeability of the wall fabric of *Escherichia coli* and *Bacillus subtilis*. J. Bacteriol. **178:**768–773.
8. **Egelseer, E., I. Schocher, M. Sara, and U. B. Sleytr.** 1995. The S-layer from *Bacillus stearothermophilus* DSM 2358 functions as an adhesion site for a high-molecular-weight amylase. J. Bacteriol. **177:**1444–1451.
9. **Gasteiger, E., C. Hoogland, A. Gattiker, S. Duvaud, M. R. Wilkins, R. D. Appel, and A. Bairoch.** 2005. Protein identification and analysis tools on the ExPASy server. *In* J. M. Walker (ed.), The proteomics protocols handbook. Humana Press, Totowa, NJ.
10. **Howorka, S., M. Sara, Y. Wang, B. Kuen, U. B. Sleytr, W. Lubitz, and H. Bayley.** 2000. Surface-accessible residues in the monomeric and assembled forms of a bacterial surface layer protein. J. Biol. Chem. **275:**37876–37886.
11. **Jakava-Viljanen, M., S. Avall-Jaaskelainen, P. Messner, U. B. Sleytr, and A. Palva.** 2002. Isolation of three new surface layer protein genes (*slp*) from *Lactobacillus brevis* ATCC 14869 and characterization of the change in their expression under aerated and anaerobic conditions. J. Bacteriol. **184:**6786–6795.
12. **Kinns, H., and S. Howorka.** 2008. The surface location of individual residues in a bacterial S-layer protein. J. Mol. Biol. **377:**589–604.
13. **Konstantinov, S. R., H. Smidt, W. M. de Vos, S. C. Bruijns, S. K. Singh, F. Valence, D. Molle, S. Lortal, E. Altermann, T. R. Klaenhammer, and Y. van Kooyk.** 2008. S layer protein A of *Lactobacillus acidophilus* NCFM regulates immature dendritic cell and T cell functions. Proc. Natl. Acad. Sci. USA **105:**19474–19479.
14. **Laemmli, U. K.** 1970. Cleavage of structural proteins during the assembly of the head of bacteriophage T4. Nature **227:**680–685.
15. **Miller, S., J. Janin, A. M. Lesk, and C. Chothia.** 1987. Interior and surface of monomeric proteins. J. Mol. Biol. **196:**641–656.
16. **Mobili, P., A. Londero, T. M. R. Maria, M. E. S. Eusébio, G. L. De Antoni, R. Fausto, and A. Gómez-Zavaglia.** 2008. Characterization of S-layer proteins of *Lactobacillus* by FTIR spectroscopy and differential scanning calorimetry. Vibrat. Spectrosc. doi:10.1016/j.vibspec.2008.07.016.
17. **Noonan, B., and T. J. Trust.** 1997. The synthesis, secretion and role in virulence of the paracrystalline surface protein layers of *Aeromonas salmonicida* and *A. hydrophila*. FEMS Microbiol. Lett. **154:**1–7.
18. **Pavkov, T., E. M. Egelseer, M. Tesarz, D. I. Svergun, U. B. Sleytr, and W. Keller.** 2008. The structure and binding behavior of the bacterial cell surface layer protein SbsC. Structure **16:**1226–1237.
19. **Prado Acosta, M., M. Mercedes Palomino, M. C. Allievi, C. Sanchez Rivas, and S. M. Ruzal.** 2008. Murein hydrolase activity in the surface layer of *Lactobacillus acidophilus* ATCC 4356. Appl. Environ. Microbiol. **74:**7824–7827.
20. **Pum, D., M. Sara, and U. B. Sleytr.** 1989. Structure, surface charge, and self-assembly of the S-layer lattice from *Bacillus coagulans* E38-66. J. Bacteriol. **171:**5296–5303.
21. **Ronka, E., E. Malinen, M. Saarela, M. Rinta-Koski, J. Aarnikunnas, and A.**

**Palva.** 2003. Probiotic and milk technological properties of *Lactobacillus brevis*. Int. J. Food Microbiol. **83:**63–74.
22. **Rost, B., G. Yachdav, and J. Liu.** 2004. The PredictProtein server. Nucleic Acids Res. **32:**W321–W326.
23. **Sambrook, J., and D. W. Russell.** 2001. Molecular cloning: a laboratory manual, 3rd ed. Cold Spring Harbor Laboratory Press, New York, NY.
24. **Sara, M., and U. B. Sleytr.** 2000. S-layer proteins. J. Bacteriol. **182:**859–868.
25. **Sara, M., and U. B. Sleytr.** 1987. Molecular sieving through S layers of *Bacillus stearothermophilus* strains. J. Bacteriol. **169:**4092–4098.
26. **Scherrer, R., and P. Gerhardt.** 1971. Molecular sieving by the *Bacillus megaterium* cell wall and protoplast. J. Bacteriol. **107:**718–735.
27. **Schuster, B., E. Gyorvary, D. Pum, and U. B. Sleytr.** 2005. Nanotechnology with S-layer proteins. Methods Mol. Biol. **300:**101–123.
28. **Sillanpaa, J., B. Martinez, J. Antikainen, T. Toba, N. Kalkkinen, S. Tankka, K. Lounatmaa, J. Keranen, M. Hook, B. Westerlund-Wikstrom, P. H. Pouwels, and T. K. Korhonen.** 2000. Characterization of the collagen-binding S-layer protein CbsA of *Lactobacillus crispatus*. J. Bacteriol. **182:**6440–6450.
29. **Sleytr, U. B., and P. Messner.** 1988. Crystalline surface layers in procaryotes. J. Bacteriol. **170:**2891–2897.
30. **Sleytr, U. B., E. M. Egelseer, N. Ilk, D. Pum, and B. Schuster.** 2007. S-layers as a basic building block in a molecular construction kit. FEBS J. **274:**323–334.
31. **Sleytr, U. B., C. Huber, N. Ilk, D. Pum, B. Schuster, and E. M. Egelseer.** 2007. S-layers as a tool kit for nanobiotechnological applications. FEMS Microbiol. Lett. **267:**131–144.
32. **Studier, F. W., A. H. Rosenberg, J. J. Dunn, and J. W. Dubendorff.** 1990. Use of T7 RNA polymerase to direct expression of cloned genes. Methods Enzymol. **185:**60–89.
33. **Tsai, C. J., S. L. Lin, H. J. Wolfson, and R. Nussinov.** 1997. Studies of protein-protein interfaces: a statistical analysis of the hydrophobic effect. Protein Sci. **6:**53–64.
34. **Vainio, U., R. A. Lauten, and R. Serimaa.** 2008. Small-angle X-ray scattering and rheological characterization of aqueous lignosulfonate solutions. Langmuir **24:**7735–7743.
35. **Ventura, M., I. Jankovic, D. C. Walker, R. D. Pridmore, and R. Zink.** 2002. Identification and characterization of novel surface proteins in *Lactobacillus johnsonii* and *Lactobacillus gasseri*. Appl. Environ. Microbiol. **68:**6172–6181.
36. **Vidgren, G., I. Palva, R. Pakkanen, K. Lounatmaa, and A. Palva.** 1992. S-layer protein gene of *Lactobacillus brevis*: cloning by polymerase chain reaction and determination of the nucleotide sequence. J. Bacteriol. **174:**7419–7427.